Bioconjugate Chemistry

Article

Iodine-124 Based Dual Positron Emission Tomography and Fluorescent Labeling Reagents for In vivo Cell Tracking

Truc Pham, Zhi Lu, Christopher Davis, Chun Li, Fangfang Sun, John Maher, and Ran Yan

Bioconjugate Chem., **Just Accepted Manuscript** • DOI: 10.1021/acs.bioconjchem.9b00799 • Publication Date (Web): 04 Mar 2020

Just Accepted

is published by the American Chemical Society. 1155 Sixteenth Street N.W., Washington, DC 20036

Iodine-124 Based Dual Positron Emission Tomography and Fluorescent Labeling Reagents for *In vivo* Cell Tracking

Authors: Truc Thuy Pham[§], Zhi Lu[*], Christopher Davis[§], Chun Li[*], Fangfang Sun[*], John Maher[#⊥//], and Ran Yan[§]

[§]King's College London, School of Biomedical Engineering and Imaging Sciences, St. Thomas' Hospital, SE1 7EH, London, United Kingdom;

[*]Department of Nuclear Medicine, First Affiliated Hospital of Dalian Medical University, People's Republic of China, 116020;

[#]King's College London, School of Cancer and Pharmaceutical Studies, Guy's Hospital, Third floor Bermondsey Wing, Great Maze Pond, London SE1 9RT, United Kingdom;

[⊥]Department of Immunology, Eastbourne Hospital, Kings Drive, Eastbourne, East Sussex, BN21 2UD, United Kingdom;

[//] Department of Clinical Immunology and Allergy, King's College Hospital NHS Foundation Trust, Denmark Hill, London SE5 9RS, United Kingdom.

Key words: cell tracking, iodine-124, positron emission tomography, multimodality imaging

ABSTRACT

Understanding the *in vivo* behavior of experimental therapeutic cells is fundamental to their successful development and clinical translation. Iodine-124 has the longest half-life (4.2 days) among the clinically used positron emitters. Consequently, this isotope offers the longest possible tracking time for directly labeled cells using positron emission tomography (PET). Herein, we have radiosynthesized and evaluated two iodine-124/fluorescein-based dual PET and fluorescent labeling reagents; namely ^{124}I-FIT-Mal and ^{124}I-FIT-$(PhS)_2$Mal for cell surface thiol bioconjugation. ^{124}I-FIT-$(PhS)_2$Mal labeled cells significantly more effectively than ^{124}I-FIT-Mal. It conjugated to various cell lines in 22%-62% labeling efficiencies with prolonged iodine-124 retention. ^{124}I-FIT-$(PhS)_2$Mal was mainly conjugated on the cell membrane confirmed by high-resolution fluorescence imaging. The migration of ^{124}I-FIT-$(PhS)_2$Mal labeled Jurkat cells was visualized in NSG mice with excellent target-to-background contrast using PET/CT over 7 days. These data demonstrate that ^{124}I-FIT-$(PhS)_2$Mal can dynamically track cell migration *in vivo* using PET/CT over a clinically relevant timeframe.

INTRODUCTION

Emerging as the fourth pillar of healthcare, cell-based therapies have shown great promise in cancer treatment,[1] stem cell regenerative medicine,[2] and immune tolerance in organ transplantation.[3] For example, adoptive transfer of chimeric antigen receptor (CAR)-engineered T-cells is a novel immunotherapy that utilizes the patient's own immune system to treat cancer.[4] One fundamental challenge in both medical research and clinical applications of cell therapies is to understand the *in vivo* behavior of the infused cells. Imaging studies can dynamically track the migration, proliferation, and final fate of the administered cells providing early insight into their safety, mechanism of action, and efficacy.[5,6] Therefore, it is essential to incorporate tracking studies at the earliest stage of clinical development in order to monitor the *in vivo* location and persistence of the cells on a patient-by-patient basis.[5,6]

To detect the initial distribution and migration of the infused cells, various direct cell labeling methods have been developed by which the therapeutic cells are labeled with a contrast reagent *in vitro*. Once inoculated into the experimental animals or patients, the movement of the labeled cells can be monitored using the corresponding imaging modality.[7-10] Positron emission tomography (PET) is a non-invasive imaging technique that can produce real-time images of radiolabeled cells *in vivo* and monitor their whole-body migration.[11] Currently, the most successful direct cell labeling method for PET involves the use of lipophilic radiometal complex, $^{89}Zr(oxine)_4$ to deposit ^{89}Zr intracellularly.[12,13] Owning to the 3.3 days half-life of ^{89}Zr, this method has been employed to track a variety of cells for several days *in vivo*. Alternatively, an ^{89}Zr-desferrioxamine-isothiocyanate bioconjugation reagent was reported to label cells through the amine groups in cell surface proteins, allowing the assessment of the distribution of the labeled cells *in vivo* for days.[14] However, when applying both of the above ^{89}Zr based cell tracking methods to monitor the experimental therapeutic cells in preclinical

settings, the ^{89}Zr leaks gradually from the labeled cells *in vivo* and deposits in bones, complicating the interpretation of PET images.[10,11,13,14]

Iodine-124 has the longest half-life ($t_{1/2}$ = 4.2 d) among the clinically used PET radioisotopes.[15] In principle, it can provide the longest possible tracking time for directly labeled cells with PET. In addition, the thyroid and stomach uptake of any free iodine-124 generated through the catabolism of the labeling reagent can be readily blocked by pre-treatment with potassium iodide. Consequently, this approach provides a low background that will improve the sensitivity and accuracy to detect the labeled cells. However, the major challenge with the use of iodine-124 based reagents for direct cell labeling is how to overcome various intracellular oxido-reductase-mediated deiodination.[15] We envisage that the deiodination can be minimized by coupling the iodine-124 on the cell surface. For this purpose, we choose thiols present in cell membrane proteins for labeling because they have been proven to be ideal functional groups in various bioconjugation applications.[16,17] To achieve both effective cell conjugation and minimum the passive diffusion of labeling reagents into cells, we hypothesize that the labeling reagents should be amphiphiles in nature. In this context, such reagents will be equipped with a lipophilic warhead to reach and react with thiols in the lipid surrounded cell surface proteins. They will also contain a negatively charged hydrophilic moiety that will repulse the negatively charged phosphate heads of the membrane lipids to minimise the labeling reagents diffusing into cells. In addition, a fluorophore will also be employed to confirm effective cell surface conjugation with fluorescence imaging. To achieve these goals, we selected two thiol-targeting moieties, maleimide and dithiophenolmaleimide for cell surface conjugation. The maleimide reacts irreversibly with the free thiols on the cell surface as demonstrated by others.[16,17] The dithiophenolmaleimide spontaneously reacts with both thiols from the reduced disulfide bridge and preserves the bridge structure in antibodies and peptides.[18,19] Although never been applied to cell labeling before, we envisaged that these

characteristics of dithiophenolmaleimide would enable it to conjugate to the cell surface proteins effectively with minimal adverse effects. We selected fluorescein as the fluorescent reporter for this application since it is used clinically in man and thus should exert negligible toxicity. Moreover, the carboxylic acid group of this hydrophilic dye is deprotonated and becomes negatively charged at physiological pH, which would retard the labeling reagent from entering cells.

Herein, using a copper mediated one-pot three-component radioiodination reaction,[20-22] we synthesized two trifunctional dual PET and fluorescent bioconjugation reagents, ^{124}I-FIT-Mal **[1]** and ^{124}I-FIT-(PhS)2Mal **[2]**. These are equipped with: (i) iodine-124 for longitudinal cell tracking with PET; (ii) a hydrophilic fluorescein moiety to balance lipophilicity and enable fluorescence cell imaging; (iii) a maleimide or dithiophenolmaleimide moiety for cell membrane protein thiol bioconjugation.

RESULTS

Synthetic chemistry and radiolabeling

Initially, the fluorescein isothiocyanate isomer I was reacted with 2-azidoethan-1-amine to generate the 5-[3-(2-azidoethyl)thioureido]-fluorescein in 82% yield. This was then converted to the 5-[3-(2-azidoethyl)ureido]-fluorescein **[3]** using pyridinium tribromide (two equivalents) in 63% yield.[23] The *N*-propargyl maleimide **[4]**[21] and the *N*-propargyl-3,4-dithiophenolmaleimide **[5]**[24] were prepared according to published methods. Subsequently, the nonradioactive reference compound of ^{124}I-FIT-Mal **[1]** was synthesized by the copper (I) mediated one-pot three-component reaction from 5-[3-(2-azidoethyl)ureido]-fluorescein **[3]**, *N*-propargyl maleimide **[4]**, and *N*-iodosuccinimide (NIS) in 56% yield. Similarly, the nonradioactive reference compound of ^{124}I-FIT-$(PhS)_2$Mal **[2]** was prepared by reacting 5-[3-

(2-azidoethyl)ureido]-fluorescein **[3]** with *N*-propargyl-3,4-dithiophenolmaleimide **[5]**, and NIS in 45% yield (**Scheme 1**).

Next, the ^{124}I-FIT-Mal **[1]** and ^{124}I-FIT-$(PhS)_2$Mal **[2]** were radiosynthesized using a one-pot three-component radioiodination reaction. The 5-[3-(2-azidoethyl)ureido]-fluorescein **[3]** and either *N*-propargyl maleimide **[4]** or *N*-propargyl-3,4-dithiophenolmaleimide **[5]** was reacted with [^{124}I]NaI in a catalytic system of $CuCl_2$/Et_3N/bathophenanthroline (10 mol%) (**Scheme 1**). Excellent radiochemical yields (RCYs) of 81±6 % (n=6) and 71±1% (n=7) were obtained for ^{124}I-FIT-Mal **[1]** and ^{124}I-FIT-$(PhS)_2$Mal **[2]** respectively, as determined by HPLC (**Figure S1 and S3**). The isolated RCYs for ^{124}I-FIT-Mal **[1]** and ^{124}I-FIT-$(PhS)_2$Mal **[2]** were 60±6% (n=6) and 53±1% (n=7), respectively. The identities of ^{124}I-FIT-Mal **[1]** and ^{124}I-FIT-$(PhS)_2$Mal **[2]** were confirmed by the co-elution with their corresponding nonradioactive reference compounds (**Figure S2 and S4**). The molar activities of ^{124}I-FIT-Mal **[1]** and ^{124}I-FIT-$(PhS)_2$Mal **[2]** were about 2.30 GBq/μmol and 1.30 GBq/μmol, respectively, when started with ~10 MBq of iodine-124. The log D for ^{124}I-FIT-Mal **[1]** and ^{124}I-FIT-$(PhS)_2$Mal **[2]** was measured by a conventional partition method between n-octanol and pH 7.4 PBS as -0.72±0.02 and 1.42±0.09 (n=6), respectively.

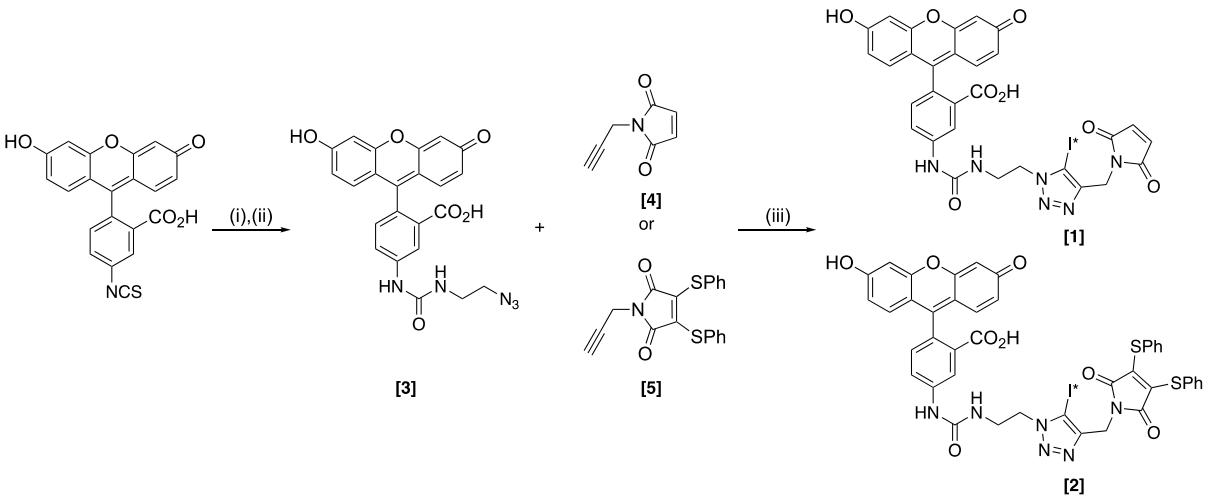

(i) 2-azidoethan-1-amine, TEA, DCM/THF, 0 ºC to RT in 3 h, 82%; (ii) pyridinium tribromide (2.0 equiv.), THF/H_2O, RT, 3 h, 63%; (iii) a) CuI, TEA, NIS, DMF, 18 h; when I*=^{127}I; or b) $CuCl_2$, TEA/TEA·HCl, bathophenanthroline (10 mol%), [^{124}I]NaI, DMF/CH_3CN/H_2O; when I*=^{124}I.

Scheme 1. Synthesis of the dual PET and fluorescent labeling reagents

Cell radiolabeling efficiency and cellular localization of the dual labeling reagents

Immortalized Jurkat human T cell lymphoma cells (5 x 10^6) were incubated with ^{124}I-FIT-Mal **[1]** or ^{124}I-FIT-$(PhS)_2$Mal **[2]** in PBS at 37 ºC for 30 min. Low labeling efficiencies of 4±1% and 11±1%, (n=3) for ^{124}I-FIT-Mal **[1]** and ^{124}I-FIT-$(PhS)_2$Mal **[2]**, respectively, were observed. In parallel experiments, Jurkat cells (5 x 10^6) were pre-treated with tris(2-carboxyethyl)phosphine (TCEP) (1.0 mM), a disulfide bridge reducing reagent in PBS for 15 min. The TCEP was then removed before incubating the cells with ^{124}I-FIT-Mal **[1]** or ^{124}I-FIT-$(PhS)_2$Mal **[2]** in PBS at 37 ºC for another 30 min. Significantly increased cell labeling efficiencies of 11±1% and 22±1%, (n=3) for ^{124}I-FIT-Mal **[1]** and ^{124}I-FIT-$(PhS)_2$Mal **[2]**, respectively, were achieved (**Figure 1A**). As ^{124}I-FIT-$(PhS)_2$Mal **[2]** labeled Jurkat cells much more effectively than ^{124}I-FIT-Mal **[1]**, it was further tested to label murine myeloma 5T33 cells and human peripheral blood T-cells. By pre-treating both cell lines (5 x 10^6) with TCEP and then incubating with ^{124}I-FIT-$(PhS)_2$Mal **[2]**, cell labeling efficiencies of 62±1% and 27±2%, (n=3), respectively, were obtained. Once again, lower cell labeling efficiencies of 44±4% and 17±1%, (n=3) for the 5T33 cells and human T-cells, respectively, were observed without TCEP pre-treatment (**Figure 1B**). To investigate the cellular localization of ^{124}I-FIT-$(PhS)_2$Mal **[2]**, Jurkat, 5T33, and human T-cells were incubated with the nonradioactive reference compound of ^{124}I-FIT-$(PhS)_2$Mal **[2]** (1.0 μM) after TCEP pre-treatment. The labeled cells

were then observed under a confocal fluorescence microscope. Green fluorescent signals were mainly distributed on the cell membrane for all three cell lines (**Figure 2**).

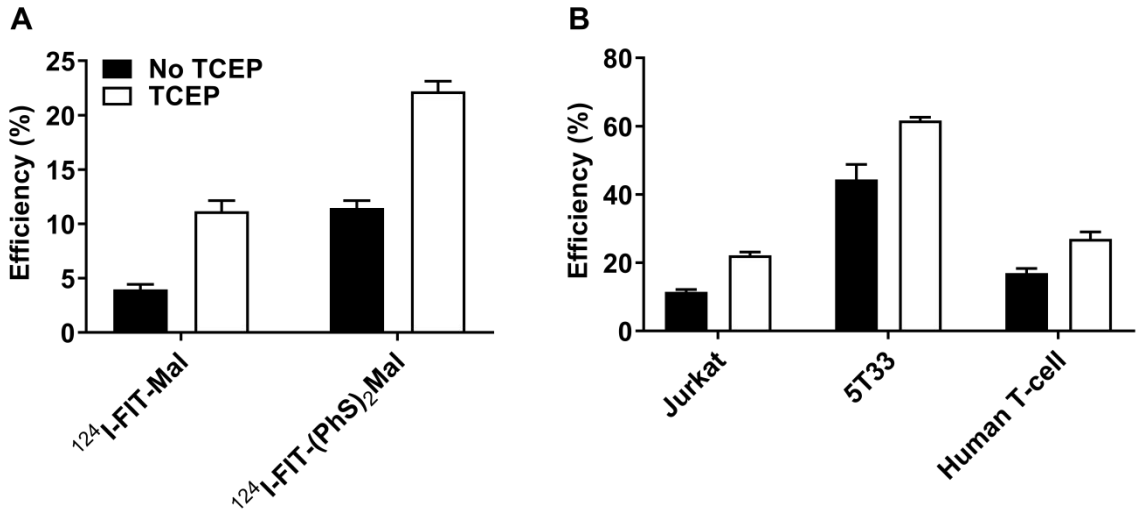

Figure 1. Cell labeling efficiencies of ^{124}I-FIT-Mal **[1]** and ^{124}I-FIT-(PhS)$_2$Mal **[2]** with Jurkat cells (**A**); cell labeling efficiencies of ^{124}I-FIT-(PhS)$_2$Mal **[2]** with Jurkat, 5T33, and human T-cells (**B**). (% incubation dose per 5 x 10^6 cells, mean±SD, n=3 independent replicates).

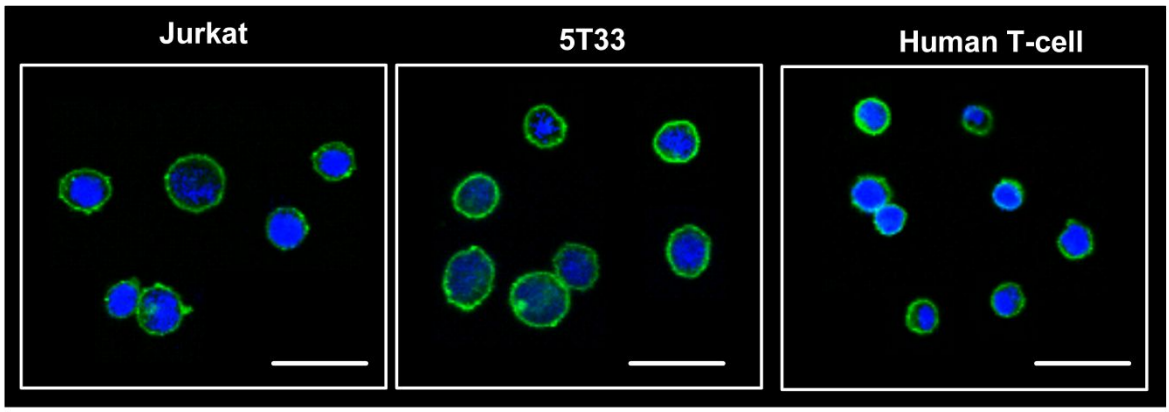

Figure 2. Confocal fluorescence images of the non-radioactive reference compound of ^{124}I-FIT-(PhS)$_2$Mal **[2]** labeled Jurkat, 5T33, and human T-cells. Nuclei were counterstained with Hoechst 33342. (Scale bar = 20 μm)

Jurkat cell ^{124}I-retention, viability, proliferation, and cytokine release post radiolabeling

We investigated the retention of iodine-124 by the ^{124}I-FIT-$(PhS)_2$Mal **[2]** labeled Jurkat cells (~100 KBq/10^6 cells) when cultured for 7 days in complete cell medium. ^{124}I-FIT-$(PhS)_2$Mal **[2]** labeled Jurkat cell viability, proliferation, and interleukin-2 (IL-2) release, was also monitored and compared with unlabeled Jurkat cells. After an initial rapid loss of about 25% radioactivity in the first 24 hours, the dissociation of iodine-124 from the labeled Jurkat cells was very slow. Notably, 65±3% (n=6) of total radioactivity was still retained in the Jurkat cells 7 days post labeling (**Figure 3A**). Cell viability was similar to the unlabeled Jurkat cells as determined by the Trypan Blue exclusion assay (**Figure 3B**). Proliferation of ^{124}I-FIT-$(PhS)_2$Mal **[2]** labeled Jurkat cells (~100 KBq/10^6 cells) was determined using the CCK-8 assay, which measures the dehydrogenase metabolic activity of proliferating cells. There is no statistically significant difference between the proliferation rates of labeled and unlabeled Jurkat cells over 7 days (**Figure 3C**). To determine Jurkat cell function post radiolabeling, ^{124}I-FIT-$(PhS)_2$Mal **[2]** labeled (~100 KBq/10^6 cells) or unlabeled Jurkat cells were treated with or without PMA/ionomycin for 24 h. The IL-2 generated was then measured using ELISA. Both labeled and unlabeled Jurkat cells produced similar amount of IL-2 upon stimulation, while little IL-2 was generated in the absence of PMA/ionomycin (day 6) (**Figure 3D**).

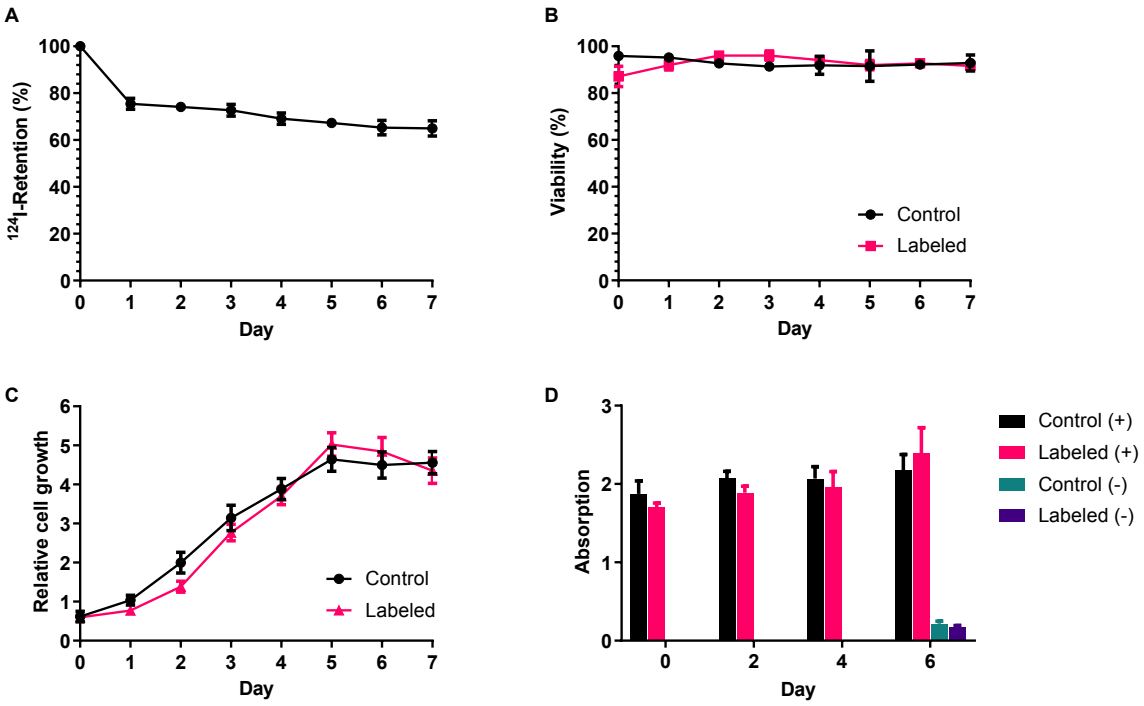

Figure 3. Retention of iodine-124 (**A**), cell viability (**B**), cell proliferation by CCK-8 assay (**C**), and IL-2 production with (+) and without (-) PMA/ionomycin activation by ELISA assay (**D**) of ^{124}I-FIT-$(PhS)_2$Mal **[2]** labeled Jurkat cells (~100 KBq/10^6 cells, mean±SD, n=6 for **A** and **B**; n=3 for **C** and **D**, independent replicates). Unlabeled cells serve as control.

In vivo cell tracking with PET imaging and biodistribution study

Subsequently, we carried out a tracking study of ^{124}I-FIT-$(PhS)_2$Mal **[2]** labeled Jurkat cells (~0.5-1.0 x 10^7 cells, ~0.5-1.0 MBq) in NSG mice (n=3) by five sequential PET/CT scans at 4 h, 24 h and 2, 5, and 7 days post intravenous (IV) injection. Radioactivity accumulated mainly in the lungs, liver, and bladder in the 4 and 24 h PET/CT images. The radioactivity gradually migrated from the lungs to the liver and cleared from the bladder in the NSG mice in the day 2, 5, and 7 PET/CT images (**Figure 4A**). After completion of PET/CT imaging on day 7, all three animals were euthanized for a biodistribution study. Radioactivity uptake of 7.90±0.88%, 2.94±0.28%, and 2.38±0.74% injected dose (ID)/g, was detected in lungs, liver, and spleen

respectively (mean±SD, n=3). Radioactivity uptake in other organs such as blood and bone etc. were all less than 1% ID/g (**Figure 5A and Table S1**). In the control group, NSG mice (n=4) received the dual labeling reagent, ^{124}I-FIT-(PhS)$_2$Mal **[2]** IV and underwent a PET/CT scan after 24 h. Most of the radioactivity had cleared from the animals and only very weak radioactivity signals were observed in the large intestine and bladder, as shown in the 24 h PET/CT image (**Figure 4B**). All four animals were euthanized after PET/CT imaging for a biodistribution study. Minimal radioactivity was detected in the lungs (0.88±0.20% ID/g), liver (0.63±0.09% ID/g), and spleen (0.44±0.05% ID/g) of these animals (**Figure 5B and table S2**).

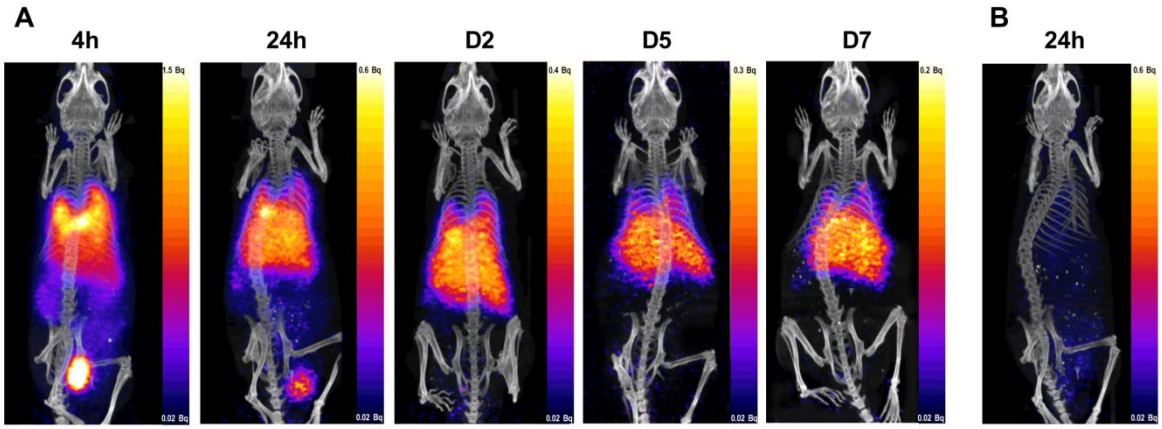

Figure 4. Representative PET/CT images of NSG mice that received either ^{124}I-FIT-(PhS)$_2$Mal **[2]** labeled Jurkat cells at 4, 24 hours, 2, 5, and 7 days (n=3) (**A**) or ^{124}I-FIT-(PhS)$_2$Mal **[2]** at 24 hours post IV injection (n=4) (**B**). All animals were treated with potassium iodide one week before and throughout the PET/CT imaging experiments.

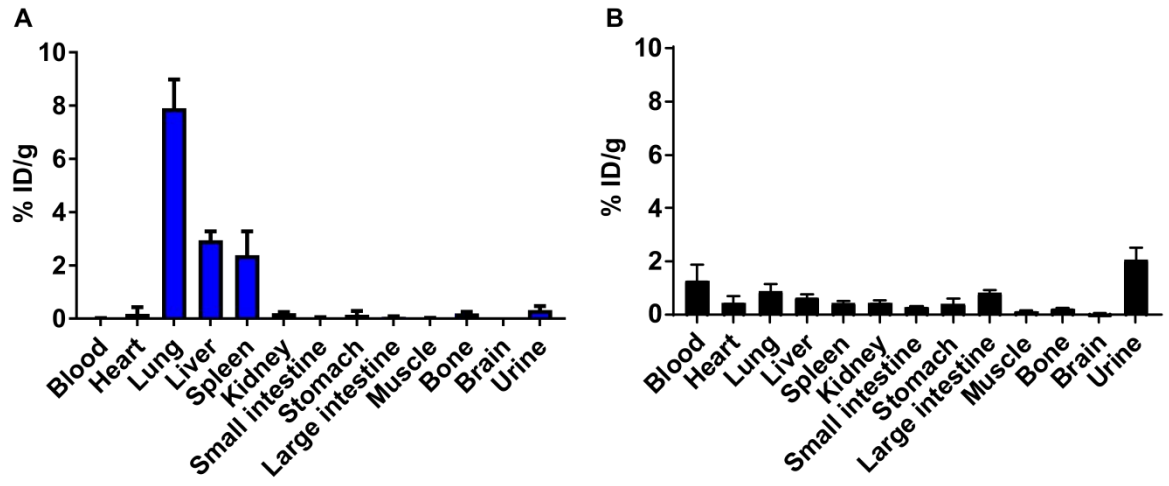

Figure 5. Biodistribution analysis of NSG mice that received either ^{124}I-FIT-$(PhS)_2$Mal **[2]** labeled Jurkat cells on day 7 post IV injection (mean±SD, n=3) (**A**) or ^{124}I-FIT-$(PhS)_2$Mal **[2]** at 24 h post IV injection (mean±SD, n=4) (**B**). All animals were treated with potassium iodide one week before until the day of the biodistribution study.

***Ex vivo* immunohistochemistry study**

Finally, we undertook immunohistology staining of liver and lung tissues harvested from NSG mice that were inoculated with ^{124}I-FIT-$(PhS)_2$Mal **[2]** labeled Jurkat cells in the PET imaging study. As controls, the liver and lungs from three NSG mice received either PBS or non-labeled Jurkat cells (~1.0 x 10^7), respectively, were collected for immunohistology staining 7 days post IV injection. All tissue sections were sequentially incubated with anti-human CD3 as the primary antibody and polymer-supported peroxidase/anti-Mouse IgG as followed by the 3,3′-diaminobenzidine (DAB) treatment. Both ^{124}I-FIT-$(PhS)_2$Mal **[2]** labeled and non-labeled Jurkat cells migrated to the liver and lung tissues from the NSG mice either used in the PET imaging study or the positive control group were stained brown in colour (**Figure 6, labeled or non-labeled Jurkat**). In contrast, the anti-human CD3 staining was negative in the liver and lung tissues from the PBS-treated NGS mice in the negative control group (**Figure 6, PBS**).

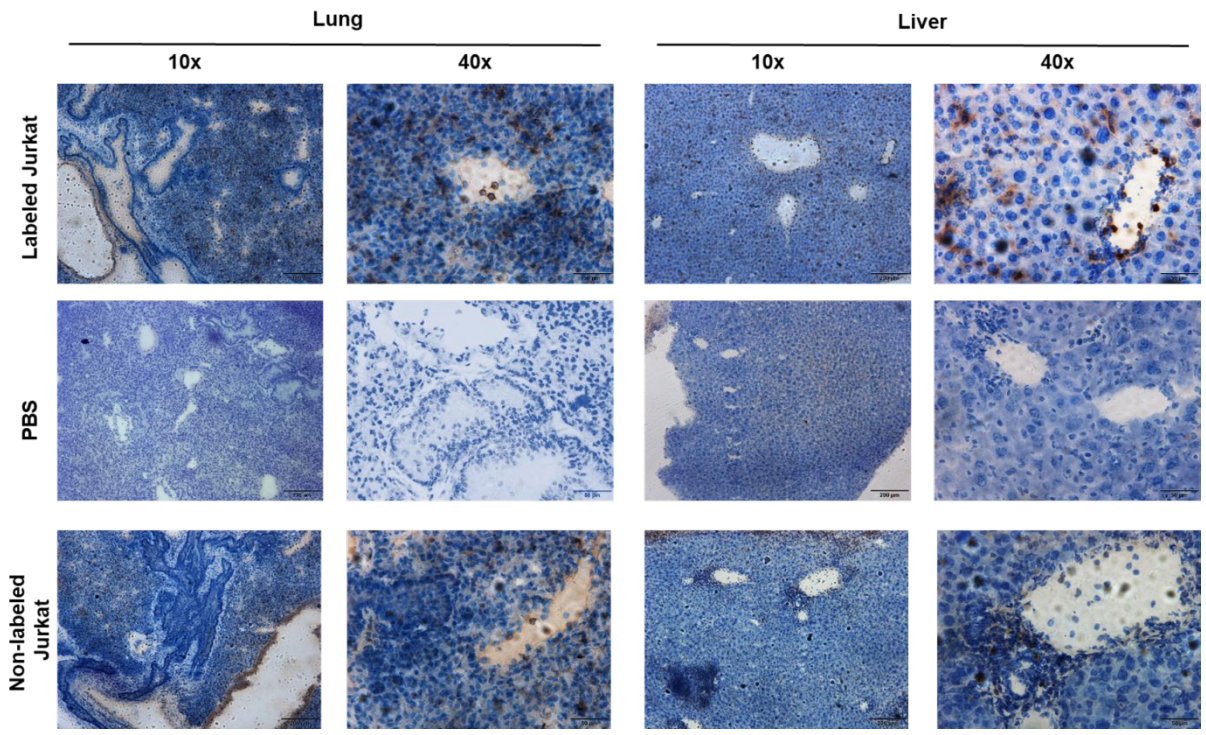

Figure 6. Representative immunohistochemistry images: liver and lung tissues collected from the NSG mice (n=3) received either ^{124}I-FIT-$(PhS)_2$Mal **[2]** labeled Jurkat cells, PBS, or non-labeled Jurkat cells 7 days post IV injection. Tissue sections were counterstained with hematoxylin. (Scale bar = 200 μm for 10x or 50 μm for 40x)

DISCUSSION

Initially, the nonradioactive reference compounds of ^{124}I-FIT-Mal **[1]** and ^{124}I-FIT-$(PhS)_2$Mal **[2]** were synthesized in moderate yields using copper mediated one-pot three-component click reactions. It proved essential to use 5-[3-(2-azidoethyl)ureido]-fluorescein **[3]** rather than its corresponding 5-[3-(2-azidoethyl)thioureido]-fluorescein formed in the first synthetic step in **Scheme 1**. No desired iodotriazoles were formed when 5-[3-(2-azidoethyl)thioureido]-fluorescein was used. This is because thioureas are susceptible to copper(II) oxidation.[25] In terms of radiosynthesis, a longer reaction time of 18 hours at RT was required to prepare ^{124}I-FIT-Mal **[1]** in both excellent RCYs and molar activity. When radiolabeling was attempted at

elevated temperature, the formation of both radioactive and non-radioactive side-products were observed, which significantly reduced the RCYs and molar activity of ^{124}I-FIT-Mal **[1]**. As iodine-124 has a half-life of 4.2 days, we decided to adopt the longer reaction time for the preparation of ^{124}I-FIT-Mal **[1]**. In contrast, ^{124}I-FIT-$(PhS)_2$Mal **[2]** was formed in both excellent RCYs and molar activity in 90 min which allows its production, cell labeling, and subsequent biological evaluation in a clinically relevant time frame. Control radiolabeling experiments in the absence of the alkynes **[4]** and **[5]** were also conducted and only the free iodine-124 was observed, which indicated that phenolic ring of the fluorescein moiety cannot be radioiodinated under the conditions used to prepare both dual labeling reagents.

Subsequently, we investigated Jurkat cell conjugation with ^{124}I-FIT-Mal **[1]** and ^{124}I-FIT-$(PhS)_2$Mal **[2]** without or with pre-treatment of the cells using a mild reducing agent, TCEP. It has been used to increase cell surface free thiols for maleimide conjugation on various cell lines including stem cells and cancer cells without adverse effect on cell functions.[16,26] The cell labeling efficiencies achieved for both ^{124}I-FIT-Mal **[1]** and ^{124}I-FIT-$(PhS)_2$Mal **[2]** were significantly improved by pre-treating the cells with TCEP which boosts the amount of cell membrane free thiols. The cell labeling efficiency for ^{124}I-FIT-$(PhS)_2$Mal **[2]** was one-fold higher than that of ^{124}I-FIT-Mal **[1]**. One possible reason is that ^{124}I-FIT-$(PhS)_2$Mal **[2]** is lipophilic which makes it more accessible to lipid surrounded cell membrane proteins. In contrast, the hydrophilic nature of ^{124}I-FIT-Mal **[1]** would be expected to repel it from the cell membrane. The general utility of ^{124}I-FIT-$(PhS)_2$Mal **[2]** for cell labeling was subsequently demonstrated by its successful conjugation to the murine myeloma 5T33 cells and to human peripheral blood T-cells. Significantly higher cell labeling efficiency was observed for the 5T33 cells compared to Jurkat cells and human T-cells. This is likely due to the higher numbers of thiols associated with 5T33 cell surface proteins as determined by the DTNB assay (supporting information). The cell membrane localization of ^{124}I-FIT-$(PhS)_2$Mal **[2]** on all three

cell lines was confirmed by confocal fluorescence imaging. Despite its lipophilic nature, the ^{124}I-FIT-$(PhS)_2$Mal **[2]** was mainly deposited on the cell membrane. This is likely resulting from the amphiphilic characteristics of this molecule. The fluorescein moiety in ^{124}I-FIT-$(PhS)_2$Mal **[2]** is negatively charged due to the deprotonation of its carboxylic acid group in PBS (pH 7.4), which repels this part of the molecule from the negatively charged cell membrane. Meanwhile, the lipophilic dithiophenolmaleimide moiety in ^{124}I-FIT-$(PhS)_2$Mal **[2]** is attracted by the cell membrane lipids. These combined forces allow ^{124}I-FIT-$(PhS)_2$Mal **[2]** to reach cell membrane protein thiols for conjugation rather than rapidly entering the cells through passive diffusion. Moreover, ^{124}I-FIT-$(PhS)_2$Mal **[2]** has shown remarkable radiolabel retention at a radioactivity level of 100 KBq/10^6 Jurkat cells, with minimum effect on cell viability. About 65% of radioactivity was still associated with the Jurkat cells *in vitro* even 7 days post radiolabeling with ^{124}I-FIT-$(PhS)_2$Mal **[2]**. This level of radioactivity retention and tolerance is comparable with that observed following ^{89}Zr(oxine)$_4$ labeling of CAR T-cells. In those cases, 40-80% of ^{89}Zr was retained for 5-7 days post labeling while tolerated radioactivity doses ranged from 30-70 KBq/10^6 cells.[10-13] Notably, about 25% of the radioactivity was lost in the first 24 hours post labeling followed by the very slow loss of radiolabel from the Jurkat cells, about 7% in six days. Due to the lipophilicity of ^{124}I-FIT-$(PhS)_2$Mal **[2]**, it would be expected to interact non-covalently with cell membrane lipids which would cause rapid dissociation of ^{124}I-FIT-$(PhS)_2$Mal **[2]** from the cells. In contrast, covalently bonded ^{124}I-FIT-$(PhS)_2$Mal **[2]** showed greater stability. In addition, faint green color was observed inside the cells in the confocal fluorescence images (**Figure 3**) indicating a small portion of ^{124}I-FIT-$(PhS)_2$Mal **[2]** did enter the cells, which could also rapidly diffuse out of the cells through passive diffusion.

Jurkat cells are leukaemic T-cells that produce IL-2 upon PMA/ionomycin stimulation. When labeled with ^{124}I-FIT-$(PhS)_2$Mal **[2]** at a radioactivity dose of about 100 KBq/10^6 cells, IL-2

production is similar to unlabeled control Jurkat cells. In addition, cell proliferation is also largely unaffected post ^{124}I-FIT-$(PhS)_2$Mal **[2]** labeling. Thus, Jurkat cell functions, in terms of IL-2 production and cell proliferation, are reserved at this radioactivity dose.

In the proof of concept *in vivo* tracking study, the migration of ^{124}I-FIT-$(PhS)_2$Mal **[2]** labeled Jurkat cells from the lungs to the liver was clearly visualized in NSG mice using five consecutive PET scans over 7 days. Spleen is a major cell migration organ we expected to observe in PET. However, the high liver radioactivity uptake and the anatomical proximity between liver and spleen completely obscured the spleen in the PET images. It is worth noting that in contrast to the high bone uptake of ^{89}Zr-based cell tracking reagents,[10,11,13,14] no bone uptake was observed in all five PET images from 4 hours until 7 days post IV injection of ^{124}I-FIT-$(PhS)_2$Mal **[2]** labeled Jurkat cells. This illustrates the superiority of this iodine-124 based strategy over the current zirconium-89 methods for direct cell labeling and long-term cell tracking with PET. As expected, thyroid and stomach uptake of iodine-124 were completely blocked by treating the animals with potassium iodide, generating a clear background for visualization of cell migration. Moreover, the initial dissociation of the labeling reagent from the Jurkat cells was observed in the 4 and 24 hour PET images, as indicated by the accumulation of radioactivity in the bladder. However, little radioactivity was observed in the bladder at later time points (2, 5, and 7 days), indicating that the labeling reagent was still associated with the Jurkat cells. These observations are in good agreement with the *in vitro* iodine-124 retention from the ^{124}I-FIT-$(PhS)_2$Mal **[2]** labeled Jurkat cells. The biodistribution study undertaken on NSG mice 7 days post inoculation of ^{124}I-FIT-$(PhS)_2$Mal **[2]** labeled Jurkat cells also provided strong evidence that the radioactivity was still concentrated in the organs to which the cells migrated. These include the lungs, liver, and spleen, with little radioactivity detected in other organs at this late time point. In contrast, in the control group that had received ^{124}I-FIT-$(PhS)_2$Mal **[2]**, both PET/CT imaging and a biodistribution study confirmed that most of the

radioactivity was cleared from the NSG mice within 24 h post IV injection. Moreover, the presence of Jurkat cells in the lungs and liver of the NSG mice that received ^{124}I-FIT-$(PhS)_2$Mal **[2]** labeled Jurkat cells from the PET imaging was further confirmed using antihuman CD3 antibody in an *ex vivo* immunohistology staining study. The distribution patterns of the ^{124}I-FIT-$(PhS)_2$Mal **[2]** labeled Jurkat cells in the lung and liver tissues are similar to the non-labeled Jurkat cells in the positive control group shown by the immunohistology staining study, which hints that the *in vivo* movability of Jurkat cells is reserved post ^{124}I-FIT-$(PhS)_2$Mal **[2]** labeling.

One possible concern is the low radioactivity dose of ^{124}I-FIT-$(PhS)_2$Mal **[2]** (~100 KBq/10^6 cells) used in the *in vivo* cell tracking study, which might be a limitation to translate this new method to clinical applications. Although there is no clinical PET imaging data to indicate the optimal radioactivity dose for directly labeled cell tracking in human, one ongoing clinical trial employs 7.4-18.5 MBq of ^{89}Zr-labeled leukocytes to track peripheral immune cell infiltration of the brain in patients with central inflammatory disorders over 6 days.[27] Moreover, in a recent ^{89}Zr-labeled natural killer (NK) cell (~1.5 x 10^8) tracking study in rhesus macaques (~6.6 Kg), clear PET images were acquired with only 2.0 MBq of radioactivity over 7 days.[28]

Given the very similar positron abundance of iodine-124 (22.5%) and zirconium-89 (22.7%), longer half-life of iodine-124 (4.2 days) than zirconium-89 (3.3 days), and excellent iodine-124 retention of ^{124}I-FIT-$(PhS)_2$Mal **[2]** labeled cells, it is a reasonable estimate that this novel iodine-124 based cell labeling method could provide a sufficient radioactivity dose (~20 MBq in 2 x 10^8 cells) for directly labeled cell tracking with PET in clinical trials.

Additionally, the latest ultra-sensitive total-body PET scanner requires a very low radioactivity dose to achieve the same signal-to-noise ratio comparing to the current clinical PET scanners. For example, in the first human PET imaging study with the EXPLORER Total-Body PET

Scanner, high quality full-body PET images were acquired by using only 25 MBq of ^{18}F-FDG (1/15 of the normal radioactivity dose) in 10 min.[29] Therefore, we anticipate that the radioactivity dose will not be a barrier to translate ^{124}I-FIT-$(PhS)_2$Mal **[2]** to clinical cell tracking.

CONCLUSION

Two dual PET and fluorescent labeling reagents, ^{124}I-FIT-Mal **[1]** and ^{124}I-FIT-$(PhS)_2$Mal **[2]** were prepared in excellent RCYs and evaluated for cell conjugation. The cell labeling efficiency of ^{124}I-FIT-$(PhS)_2$Mal **[2]** is significantly better than ^{124}I-FIT-Mal **[1]**. ^{124}I-FIT-$(PhS)_2$Mal **[2]** was used to successfully label various cell lines through their membrane thiols in 22%-62% labeling efficiency with prolonged radiolabel retention. Cell membrane localization of ^{124}I-FIT-$(PhS)_2$Mal **[2]** was confirmed by confocal fluorescence imaging. Longitudinal monitoring of the *in vivo* distribution and migration of ^{124}I-FIT-$(PhS)_2$Mal **[2]** labeled Jurkat cells was achieved with PET/CT imaging over 7 days with excellent target-to-background contrast. These promising results warrant future studies in which therapeutic cells such as anti-cancer CAR T-cells will be labeled with ^{124}I-FIT-$(PhS)_2$Mal **[2]** for *in vivo* tracking using PET/CT.

EXPERIMENTAL SECTION

Synthetic chemistry and radiochemistry

General information

^{1}H and ^{13}C NMR spectra were recorded at RT on a Bruker Avance 400 instrument operating at the frequency of 400 MHz for ^{1}H and 100 MHz for ^{13}C. Chemical shifts are reported in ppm relative to chloroform (δ 7.26, s), dimethyl sulfoxide (δ 2.48, m) or methanol (δ 3.49, s and

1.09, s) and coupling constants (J) are given in Hertz. HPLC analysis was performed with an Agilent 1200 HPLC system equipped with a 1200 series diode array detector and a 1200 series fluorescence detector (G1321A). Radio-HPLC analysis was performed with an Agilent 1200 HPLC system equipped with a series diode array detector and Raytest GABI Star radioactivity detector. The radiochemical purity of ^{124}I-FIT-Mal and ^{124}I-FIT-$(PhS)_2$Mal was determined using radioHPLC and it is greater than 95% (**Figure S2 and S4**). Reductant free [^{124}I]NaI was purchased from Perkin Elmer (product number NEZ309) in 0.02 M NaOH (pH 14) aqueous solution. All reagents were purchased from Sigma-Aldrich and were used without further purification.

5-[3-(2-azidoethyl)thioureido]-fluorescein

To a solution of fluorescein isothiocyanate isomer I (0.50 g, 1.28 mmol) in anhydrous THF (45 mL) at 0 ºC, the freshly prepared 2-aminoethyl azide[21] solution in DCM (5 mL) was added under an atmosphere of N_2, followed by triethylamine (0.18 ml, 1.28 mmol). The reaction solution was warmed to RT while stirring for 3 h. The solvents were removed in vacuo and the residue was purified by column chromatography (DCM, 0.1%TFA → DCM, 5% MeOH, 0.1% TFA) to afford the title compound as a yellow solid (0.51 g, 82%).

^{1}H NMR (400 MHz, MeOH-*d4*): δ 8.17 (1H, s, Ar-CH), 7.79 (1H, J = 8.0 Hz, d, Ar-CH), 7.19 (1H, J = 8.0 Hz, d, Ar-CH), 6.72 (2H, J = 8.0 Hz, d, Ar-CH), 6.68 (2H, J = 4.0 Hz, d, Ar-CH), 6.58 (2H, J = 8.0 Hz, J' = 4.0 Hz, dd, Ar-CH), 3.83 (2H, J = 12.0 Hz, t, CH_2), 3.61 (2H, J = 12.0 Hz, t, CH_2); ^{13}C NMR (100 MHz, DMSO-*d6*) δ 180.8, 168.7, 162.9, 152.9, 141.0 129.3, 128.1, 125.1, 118.2, 114.4, 110.4, 102.3, 49.3, 40.6; HRMS (EI, $^m/_z$) $[M+H]^+$: calc. for $C_{23}H_{18}N_5O_5S$ 476.1029; found: 476.1028.

5-[3-(2-azidoethyl)ureido]-fluorescein [3]

To a solution of 5-[3-(2-azidoethyl)thioureido]-fluorescein (140 mg, 0.3 mmol) and pyridinium tribromide (190 mg, 0.60 mmol) in THF (4 mL), water (2 mL) was added dropwise and the resulting solution was stirred at RT for 3 h. The reaction mixture was filtered. Water (20 mL) was added to the filtrate and extracted with EtOAc (3 x 20 mL). The organic extracts were dried over $MgSO_4$ and evaporated under vacuo. Purification by column chromatography (0-5% MeOH in DCM, 0.1%TFA) yielded the title compound as an orange solid (81 mg, 63%).

^{1}H NMR (400 MHz, DMSO-*d6*): δ 10.08 (2H, s, OH), 9.11 (1H, s, NH), 8.15 (1H, s, Ar-CH), 7.63 (1H, J = 8.0, d, Ar-CH), 7.13 (1H, J = 8.0 Hz, d, Ar-CH), 6.67 (2H, s, Ar-CH), 6.56-6.51 (5H, m, Ar-CH x 4 and NH), 3.46–3.43 (2H, m, CH_2), 3.36–3.33 (2H, m, CH_2); ^{13}C NMR (100 MHz, DMSO-*d6*) δ 169.3, 159.9, 155.6, 152.4, 145.4, 142.5, 129.5, 127.5, 125.7, 124.7, 113.0, 112.2, 110.4, 102.7, 83.4, 51.1, 40.0; HRMS (EI, $^m/_z$) $[M+H]^+$: calc. for $C_{23}H_{18}N_5O_6$ 460.1257; found: 460.1267.

Non-radioactive reference compounds of the dual PET and fluorescent labeling reagents

To a solution of copper(I) iodide (14.5 mg, 76.2 µmol) and triethylamine (10.6 µl, 76.2 µmol) in dry DMF (1.0 mL), bathophenanthroline (2.5 mg, 7.62 µmol) was added under an atmosphere of argon, followed by either *N*-propargyl maleimide **[4]** or *N*-propargyl-3,4-dithiophenolmaleimide **[5]** (76.2 µmol), *N*-iodosuccinimide (25.7 mg, 114.4 µmol), and the 5-[3-(2-azidoethyl)ureido]-fluorescein **[3]** (76.2 µmol). The resulting mixture was stirred at RT for 18 h. Water (10 mL) was added and the product mixture was extracted with EtOAc (3 x 15 mL). The organic extracts were washed with brine and dried over $MgSO_4$. After filtration, the solvent was removed under vacuo.

^{127}I-FIT-Mal **[1]**: the crude mixture was washed with cold diethyl ether (3 x 10 mL) and then purified with flash column chromatography on silica (0-10% MeOH in DCM) to yield the title

compound as an orange solid. (31mg, 56%). ^{1}H NMR (400 MHz, DMSO-*d6*) δ 10.11 (2H, s, OH), 9.24 (1H, s, NH), 8.14 (1H, s, Ar-H), 7.61 (1H, *J* = 8.0 Hz, d, Ar-H), 7.12 (2H, s, CH=CH), 7.10 (1H, *J* = 8.0 Hz, d, Ar-H), 6.68 (2H, s, Ar-H) 6.58 – 6.53 (5H, m, Ar-CH x 4 and NH), 4.62 (2H, s, CH_2), 4.47 (2H, *J* = 6.0 Hz, t, CH_2); 3.57 (2H, *J* = 6.0 t, CH_2). ^{13}C NMR (100 MHz, DMSO-*d6*) δ 170.8, 169.3, 159.9, 155.6, 152.4, 146.1, 145.4, 142.5, 135.3, 130.0, 129.5, 127.4, 125.7, 124.6, 113.0, 112.2, 110.4, 102.7, 83.5, 83.4, 55.4, 50.3, 46.0. HRMS (EI, $^{m}/_{z}$) $[M+H]^+$: calc. for $C_{30}H_{22}IN_6O_8$ 721.0544; found 721.0533.

^{127}I-FIT-$(PhS)_2$Mal **[2]**: the crude product was purified by C-18 reverse phase flash column chromatography using Combiflash (5 to 95% MeOH in water) to afford the title compound as an orange solid (32 mg, 45%).

^{1}H NMR (400 MHz, DMSO-*d6*) δ 9.15 (1H, s, NH), 8.14 (1H, *J* = 2.0 Hz, d, Ar-H), 7.60 (1H, *J* = 8.0 Hz, *J'* = 2.0 Hz, dd, Ar-H), 7.34 - 7.23 (10H, m, Ph x 2), 7.11 (1H, *J* = 8.0 Hz, d, Ar-H), 6.67 (2H, *J*= 2.0, d, Ar-H), 6.74 – 6.43 (4H, m), 6.48 (1H, *J* = 11.0 Hz, t, NH), 4.65 (2H, s), 4.48 (2H, *J* = 6.0 Hz, t); 3.58 (2H, *J* = 11.0 Hz, *J'* = 6.0 Hz, q). ^{13}C NMR (100 MHz, DMSO-*d6*) δ 168.9, 165.7, 159.4, 155.0, 151.9, 145.1, 144.9, 142.0, 135.8, 130.9, 130.9, 129.1, 129.0, 128.9, 128.1, 126.9, 125.3, 124.2, 112.5, 111.7, 109.9, 102.1, 82.9, 82.8, 49.8, 34.4; HRMS (EI, $^{m}/_{z}$) $[M+H]^+$: calc. for $C_{42}H_{30}IN_6O_8S_2$ 937.0611, found: 937.0635.

Radiolabeling

Copper (II) chloride (3.4 mg, 25.3 μmol), triethylamine (4.4 μL, 31.5 μmol, 1.38 equiv.), and bathophenanthroline (850 μg, 2.5 μmol, 10 % mol) were mixed in anhydrous acetonitrile (500 μL). The resulting suspension (62.5 μL) was added to either *N*-propargyl maleimide **[4]** or *N*-propargyl-3,4-dithiophenolmaleimide **[5]** (3.1 μmol) in anhydrous DMF (62.5 μL). The resulting red suspension (40 μL) was added to a mixture of 5-[3-(2-azidoethyl)ureido]-

fluorescein **[3]** (1.0 μmol) and triethylamine hydrochloride (TEA·HCl) (16.5 μg, 0.12 μmol) in acetonitrile (20 μL) and [^{124}I]NaI (~12 MBq) in 0.02 M NaOH solution (6.0 μL).

^{124}I-FIT-Mal **[1]**: after incubation at RT for 18 h, the reaction mixture was quenched with DMSO (100 μL) followed by water/MeOH (4:1, 1.0 mL). The resulting solution was purified by HPLC using a ZORBAX column (300SB-C18, 9.4 X 250 mm, 5 μm) with the following eluent: water (0.1% TFA) as solvent A and methanol (0.1% TFA) as solvent B, went from 30% B to 47.5% B in 5 min, kept at 47.5% B for 20 min, went to 90% B in 5 min, and went back to 30% B in 5 min with a flow rate of 2.5 mL/min. The retention time of the title compounds was 20.4 min.

^{124}I-FIT-$(PhS)_2$Mal **[2]**: after incubation at 60 ºC for 90 min, the reaction mixture was quenched with DMSO (100 μL) followed by water/MeOH (4:1, 1.0 mL). The resulting solution was purified by HPLC using a ZORBAX column (300SB-C18, 9.4 X 250 mm, 5 μm) with the following eluent: water (0.1% TFA) as solvent A and methanol (0.1% TFA) as solvent B, went from 70% B to 75% B in 15 min, increased to 90% B in 5 min, and went back to 70% B in 5 min with a flow rate of 2.5 mL/min. The retention time of the title compounds was 12.4 min.

The identity of both dual labeling reagents was confirmed by co-eluting with their corresponding non-radioactive reference compounds (**Figure S2 and S4**). Formulation: the HPLC eluent containing the dual labeling reagent was diluted to 15% MeOH in water and was loaded on either a pre-conditioned Waters C18 light Sep-Pak cartridge for ^{124}I-FIT-Mal **[1]** or Waters t-C18 Sep-Pak cartridge for ^{124}I-FIT-$(PhS)_2$Mal **[2]**. After washing with water (5 mL), the dual labeling reagent was released using EtOH. The EtOH was removed by a stream of N_2 and then the dual labeling reagent was re-dissolved in DMSO for further use.

Log D measurement

The lipophilicity of ^{124}I-FIT-Mal **[1]** and ^{124}I-FIT-$(PhS)_2$Mal **[2]** was determined by a conventional partition method between n-octanol and PBS, pH 7.4. The n-octanol was saturated with PBS before use. The ^{124}I-FIT-Mal **[1]** or ^{124}I-FIT-$(PhS)_2$Mal **[2]** (1 µL, ~2 KBq) in DMSO was added to a mixture of PBS (200 µL) and n-octanol (200 µL) in a 1.5 mL Eppendorf vial (n=6). The mixture was vigorously agitated at RT for 5 min and then centrifuged at 3000 g for 10 min. A 100 µL aliquot from each layer was drawn for measurement in a gamma counter.

Cell culture

T-cells were isolated from peripheral blood samples taken from healthy volunteers aged 18 – 45 (KCL ethics approval: HR-18/19-8846) *via* Ficoll separation. Blood was slowly added to a 50 mL Falcon tube containing 15 mL of Ficoll-Paque (GE Healthcare) solution and spun in a centrifuge at 500 g for 25 minutes. The peripheral blood mononuclear cell layer was extracted and the cells were washed twice with PBS and prepared for activation. Cells were re-suspended in RPMI 1640 cell growth medium at a concentration of 3 x 10^6 cells/mL and plated on a 6-well plate (4 mL per well). T-cells were activated with 5 µg/mL of phytohemagglutinin (PHA-L, Sigma-Aldrich). IL-2 (100 U/mL, PeproTech) and fresh medium were added every 2-3 days.

Jurkat and murine myeloma 5T33 (generous gift from Dr Yolanda Calle-Patino) cells were cultured in RPMI-1640 medium supplemented with 10% FBS, 200 U/L penicillin, 0.1 g/L streptomycin and 2 mM L-glutamine. The cell concentration was maintained in 1 x 10^5~1 x 10^6 cells/mL in a humidified chamber containing 5% CO_2 at 37 ^oC.

Cell labeling

For ^{124}I-FIT-Mal **[1]** and ^{124}I-FIT-$(PhS)_2$Mal **[2]**: suspension cells (5 x 10^6, n=3) were either treated with TCEP (1.0 mL, 1.0 mM) in PBS or PBS (1 mL) only and kept in RT for 15 min before washing with PBS (3 x 1.0 mL). The cells were re-suspended in PBS (0.5 mL) and

followed by the addition of ^{124}I-FIT-Mal **[1]** or ^{124}I-FIT-$(PhS)_2$Mal **[2]** (~3 MBq**)** in DMSO (5 µL). After incubation at 37 °C for another 30 min, the cells were centrifuged (1200 rpm, 5 min), the supernatants were transferred to new Eppendorf tubes. The pellets were further rinsed with PBS (2 x 0.5 mL) before being transferred to new Eppendorf tubes and re-cultivated in complete medium. To determine the cell labeling efficiency, the supernatants and the washes for each sample were combined. The pellets, supernatants, and Eppendorf tubes used for cell labeling were measured by a Capintec CRC®-25R dose calibrator (Capintec Inc, USA).

For the non-radioactive reference compound of ^{124}I-FIT-$(PhS)_2$Mal **[2]**: suspension cells (2 x 10^6, n=3) were treated with TCEP (1.0 mL, 1.0 mM) in PBS and incubated at RT for 15 min before being washed with PBS (3 x 1.0 mL) to remove TCEP. The cells were then re-suspended in PBS (1.0 mL) and the nonradioactive reference compound of ^{124}I-FIT-$(PhS)_2$Mal **[2]** in DMSO (0.5 µL, 2.0 mM) was added to achieve the final concentration of 1.0 µM. The cells were incubated at 37 °C for another 30 min. Hoechst 33342 in DMSO (2 µL, 250 µM) was added to the cells 5 min before the end of incubation. The cells were centrifuged (1200 rpm, 5 min), the supernatants were removed and the pellets were further rinsed with PBS (3 x 1.0 mL). The sample was then fixed with 4% paraformaldehyde at RT for 10 min in darkness. Following fixation step, the cells were washed with PBS (3 x 1.0 mL) and re-suspended in PBS (50 µL). The cell sample (10 µL) was mounted on a microscopic glass slide, covered with a coverslip, and sealed with transparent nail enamel. High-resolution confocal fluorescence images were obtained with a Leica TCS SP5 II confocal microscope (Leica Microsystems Ltd) system and processed using LAS AF Lite (ver 2.6.3, build 8173, Leica Microsystems Ltd). Excitation/emission wavelengths were 495/517 nm and UV/455 nm for FITC and Hoechst 33342, respectively.

Iodine-124 retention and cell viability post radiolabeling

Both the ^{124}I-FIT-$(PhS)_2$Mal **[2]** labeled and untreated control Jurkat cells were maintained at 0.2-1.0 x 10^6 cells/mL in complete cell media. To determine the retention of iodine-124, the ^{124}I-FIT-$(PhS)_2$Mal **[2]** labeled Jurkat cells (0.5 mL) was collected daily. After centrifugation at 1500 rpm for 5 min, the supernatant and the pellet were separated and gamma counted using a Wallac Wizard™ 1480 automatic gamma counter (Perkin Elmer, USA). Trypan Blue was employed to measure the cell viability. The number of live and dead cells were counted and the percentage of the cell viability was calculated. The experiments were conducted in triplicates. The data were analyzed using GraphPad Prism 7 software.

Cell proliferation assay

The effect of radiolabeling on cellular proliferation was assessed using the Cell Counting Kit-8 (CCK-8). Both the ^{124}I-FIT-$(PhS)_2$Mal [2] labeled (~100 KBq/10^6 cells) and unlabeled Jurkat cells were maintained in complete cell media at an initial concentration of 0.2 x 10^6 cells/mL. The culture medium was replaced daily. The CCK-8 assay was performed in triplicate daily for 7 days. In general, 10 µL of the CCK-8 solution was added to 100 µL aliquots of either the labeled or unlabeled Jurkat cells; then the absorbance at 450 nm was measured with a SpectraMax 190 absorbance microplate reader (Molecular Devices, USA) after incubation at 37 °C for 3 hours. The experiments were conducted in triplicate. Results are presented as mean ± SD.

Cell function assay

Both the ^{124}I-FIT-$(PhS)_2$Mal [2] labeled (~100 KBq/10^6 cells) and unlabeled Jurkat cells were maintained at 0.2-1.0 x 10^6 cells/mL in complete cell media. The labeled or unlabeled Jurkat cells (1.0 x 10^6 cells/mL) were seeded into a 96 well-plate (100 µL/well) in triplicate. 12-*O*-tetradecanoylphorbol 13-acetate (PMA) (30 ng/mL)/ionomycin (0.75 µg/mL) or cell media as

negative control were added to the Jurkat cells and incubated for 24 hrs. Supernatant samples (30 µL/well) were analysed by ELISA using human IL-2 Ready-SET-Go ELISA® kits from eBioscience (Hatfield, UK), according to the manufacturer's instructions. Absorbance at 450 nm and 570 nm were recorded using a SpectraMax 190 absorbance microplate reader and mean absorbance of each sample at 450 nm was subtracted from absorbance at 570 nm. This protocol was repeated every other day for 6 days. The experiments were conducted in triplicates. Results are presented as the mean ± SD.

In vivo PET imaging and biodistribution studies

All animal experiments complied with the ARRIVE guidelines, the Animals (Scientific Procedures) Act (UK 1986), and Home Office (UK) guidelines and were conducted under a Home Office licence (P9C94E8A4) with local ethical approval by the KCL College Research Ethics Committee (CREC).

Preclinical PET/CT images were acquired using a NanoScan PET/CT (Mediso, Budapest, Hungary) scanner with mice under 2% isoflurane in oxygen anesthesia. Drinking water containing potassium iodide (0.1%, w/v) were provided to male NSG mice (n=7) for one week before and throughout the PET/CT imaging experiments. On day eight, they were randomly divided into two groups received either the ^{124}I-FIT-$(PhS)_2$Mal **[2]** labeled Jurkat cells (~0.5-1.0 x 10^7, ~0.5-1.0 MBq, n=3) in PBS or ^{124}I-FIT-$(PhS)_2$Mal **[2]** (~0.7 MBq, n=4) in PBS (100 µL) with 5% DMSO *via* tail vein injection. PET scanning was performed for 60 min either at 4, 24 h, 2, 4, and 7 days post Jurkat cell inoculation or at 24 h post ^{124}I-FIT-$(PhS)_2$Mal **[2]** injection followed by a 15 min CT scan. All PET/CT data were reconstructed with the Monte Carlo-based full-3D iterative algorithm Tera-Tomo (Mediso Medical Imaging Systems, Budapest, Hungary). Raw PET data were reconstructed into 60-min bins using reconstruction settings (4 iterations, 6 subsets, 0.4×0.4×0.4 mm^3 voxel size) as well as intercrystal scatter

correction. All reconstructed data were analyzed with VivoQuant software (v3.0, inviCRO, LLC, Boston, USA). All animals were euthanized by cervical dislocation at the end of the last PET/CT scan. The major thoracoabdominal organs, brain, blood, urine, left femur, and thigh muscle were harvested, weighed, and gamma-counted. The radioactivity in each organ was expressed as % ID/g. The total injected dose was defined as the sum of the whole body counts excluding the tail.

Immunohistochemistry

Three cryosections (10 μm thick) were prepared from the liver and lung of NSG mice (n=3) one week after receiving either ^{124}I-FIT-$(PhS)_2$Mal **[2]** labeled Jurkat cells from above PET imaging study, PBS, or non-labeled Jurkat cells (~1.0 x 10^7). These tissue sections were fixed with acetone and dried in air. The tissue sections were then sequentially incubated with anti-CD3 primary antibody (clone LN10, Leica #CD3-565-L-CE) and Polymer-supported peroxidase and anti-Mouse IgG followed by DAB treatment (MaxVision^{TM}2 HRP-Polymer anti-Mouse IHC Kit) and finally stained with hematoxylin. The tissue sections were then observed under an Olympus DP73 digital microscope.

ABBREVIATIONS

Bq: becquerel; CT: computed tomography; IV: intravenous; %ID/g: percentage injected dose per gram tissue; PBS: phosphate buffered saline; PET: positron emission tomography; NIS: *N*-iodosuccinimide; RCYs: radiochemical yields; RT: room temperature; TCEP: tris(2-carboxyethyl)phosphine; TEA·HCl: triethylamine hydrochloride.

AUTHOR INFORMATION

Corresponding authors

Ran Yan

King's College London, School of Imaging Sciences and Biomedical Engineering, St. Thomas' Hospital, SE1 7EH, London, United Kingdom; Email: ran.yan@kcl.ac.uk; Telephone: 00442071889613

ACKNOWLEDGMENTS

Truc Thuy Pham received a Rosetrees Trust PhD studentship (M545) to support this work. Zhi Lu received a funding from Natural Science Foundation of Liaoning Province, China (20180530048) for support of this work. Christopher Davis received an EPSRC PhD studentship (EP/R513064/1) to support this work. The research was funded/supported by the National Institute for Health Research (NIHR) Biomedical Research Centre based at Guy's and St Thomas' NHS Foundation Trust and King's College London, the Wellcome/EPSRC Centre for Medical Engineering at King's College London [WT 203148/Z/16/Z], the King's College London and UCL Comprehensive Cancer Imaging Centre funded by CRUK and EPSRC in association with the MRC and DoH (England), the Experimental Cancer Medicine Centre at King's College and the King's Health Partners/ King's College London Cancer Research UK Cancer Centre. The views expressed are those of the authors and not necessarily those of the NHS, the NIHR, or the DoH. PET scanning equipment was funded by an equipment grant from the Wellcome Trust.

Note

John Maher is Chief Scientific Officer of Leucid Bio, which is a spinout company focused on development of cellular therapeutic agents. The other authors declare no competing financial interest.

ASSOCIATED CONTENT

Supporting information

- HPLC chromatograms including the crude radioiodination mixture of dual labeling reagents and co-elution with their nonradioactive reference compounds;
- Cell surface thiol determination;
- A table for the ^{124}I-FIT-$(PhS)_2$Mal **[2]** labeled Jurkat cell biodistribution data from NSG mice 7 days post IV injection;
- A table for the ^{124}I-FIT-$(PhS)_2$Mal **[2]** biodistribution data from NSG mice 24 hours post IV injection;
- ^{1}H and ^{13}C NMR spectra for all compounds prepared.

REFERENCES

(1) Hinrichs, C. S.; Rosenberg, S. A. Exploiting the Curative Potential of Adoptive T-Cell Therapy for Cancer. *Immunol. Rev.* **2014**, *257* (1), 56–71.

(2) Trounson, A.; McDonald, C. Stem Cell Therapies in Clinical Trials: Progress and Challenges. *Cell Stem Cell* **2015**, *17* (1), 11–22.

(3) Scalea, J. R.; Tomita, Y.; Lindholm, C. R.; Burlingham, W. Transplantation Tolerance Induction: Cell Therapies and Their Mechanisms. *Front. Immunol.* **2016**, *7*, Article 87.

(4) Feins, S.; Kong, W.; Williams, E. F.; Milone, M. C.; Fraietta, J. A. An Introduction to Chimeric Antigen Receptor (CAR) T-Cell Immunotherapy for Human Cancer. *Am. J. Hematol.* **2019**, *94* (S1), S3–S9.

(5) Kircher, M. F.; Gambhir, S. S.; Grimm, J. Noninvasive Cell-Tracking Methods. *Nat. Rev. Clin. Oncol.* **2011**, *8* (11), 677–688.

(6) Martinez, O.; Sosabowski, J.; Maher, J.; Papa, S. New Developments in Imaging Cell-Based Therapy. *J. Nucl. Med.* **2019**, *60* (6), 730–735.

(7) Hughes, D. K. Nuclear Medicine and Infection Detection: The Relative Effectiveness of Imaging with ^{111}In-Oxine-, ^{99m}Tc-HMPAO-, and ^{99m}Tc-Stannous Fluoride Colloid-Labeled Leukocytes and with ^{67}Ga-Citrate. *J. Nucl. Med. Technol.* **2003**, *31* (1), 196–201.

(8) Bulte, J. W. M. *In Vivo* MRI Cell Tracking: Clinical Studies. *AJR. Am. J. Roentgenol.* **2009**, *193* (2), 314–325.

(9) Swirski, F. K.; Berger, C. R.; Figueiredo, J. L.; Mempel, T. R.; von Andrian, U. H.; Pittet, M. J.; Weissleder, R. A Near-Infrared Cell Tracker Reagent for Multiscopic *In Vivo* Imaging and Quantification of Leukocyte Immune Responses. *PLoS One* **2007**, *2* (10), e1075.

(10) Man, F.; Lim, L.; Volpe, A.; Gabizon, A.; Shmeeda, H.; Draper, B.; Parente-Pereira, A. C.; Maher, J.; Blower, P. J.; Fruhwirth, G. O.; et al. *In Vivo* PET Tracking of ^{89}Zr-Labeled Vγ9Vδ2 T Cells to Mouse Xenograft Breast Tumors Activated with Liposomal Alendronate. *Mol. Ther.* **2019**, *27*, 219–229.

(11) Weist, M. R.; Starr, R.; Aguilar, B.; Chea, J.; Miles, J. K.; Poku, E.; Gerdts, E.; Yang, X.; Priceman, S. J.; Forman, S. J.; et al. PET of Adoptively Transferred Chimeric Antigen Receptor T Cells with ^{89}Zr-Oxine. *J. Nucl. Med.* **2018**, *59* (10), 1531–1537.

(12) Sato, N.; Wu, H.; Asiedu, K. O.; Szajek, L. P.; Griffiths, G. L.; Choyke, P. L. (89)Zr-Oxine Complex PET Cell Imaging in Monitoring Cell-Based Therapies. *Radiology* **2015**, *275* (2), 490–500.

(13) Charoenphun, P.; Meszaros, L. K.; Chuamsaamarkkee, K.; Sharif-Paghaleh, E.; Ballinger, J. R.; Ferris, T. J.; Went, M. J.; Mullen, G. E. D.; Blower, P. J. [^{89}Zr]Oxinate$_4$ for Long-Term in Vivo Cell Tracking by Positron Emission Tomography. *Eur. J. Nucl. Med. Mol. Imaging* **2015**, *42* (2),

(14) Bansal, A.; Pandey, M. K.; Demirhan, Y. E.; Nesbitt, J. J.; Crespo-Diaz, R. J.; Terzic, A.; Behfar, A.; DeGrado, T. R. Novel ^{89}Zr Cell Labeling Approach for PET-Based Cell Trafficking Studies. *EJNMMI Res.* **2015**, *5*, Article 19.

(15) Belov, V. V.; Bonab, A. A.; Fischman, A. J.; Heartlein, M.; Calias, P.; Papisov, M. I. Iodine-124 as a Label for Pharmacological PET Imaging. *Mol. Pharm.* **2011**, *8*, 736–747.

(16) Kim, H.; Shin, K.; Park, O. K.; Choi, D.; Kim, H. D.; Baik, S.; Lee, S. H.; Kwon, S.-H.; Yarema, K. J.; Hong, J.; et al. General and Facile Coating of Single Cells via Mild Reduction. *J. Am. Chem. Soc.* **2018**, *140* (4), 1199–1202.

(17) Stephan, M. T.; Moon, J. J.; Um, S. H.; Bershteyn, A.; Irvine, D. J. Therapeutic Cell Engineering with Surface-Conjugated Synthetic Nanoparticles. *Nat. Med.* **2010**, *16* (9), 1035–1041.

(18) Schumacher, F. F.; Nunes, J. P. M.; Maruani, A.; Chudasama, V.; Smith, M. E. B.; Chester, K. A.; Baker, J. R.; Caddick, S. Next Generation Maleimides Enable the Controlled Assembly of Antibody-Drug Conjugates via Native Disulfide Bond Bridging. *Org. Biomol. Chem.* **2014**, *12* (37), 7261–7269.

(19) Schumacher, F. F.; Nobles, M.; Ryan, C. P.; Smith, M. E. B.; Tinker, A.; Caddick, S.; Baker, J. R. In Situ Maleimide Bridging of Disulfides and a New Approach to Protein PEGylation. *Bioconjug. Chem.* **2011**, *22* (2), 132–136.

(20) Yan, R.; El-Emir, E.; Rajkumar, V.; Robson, M.; Jathoul, A. P.; Pedley, R. B.; Årstad, E. One-Pot Synthesis of an ^{125}I-Labeled Trifunctional Reagent for Multiscale Imaging with Optical and Nuclear Techniques. *Angew. Chemie - Int. Ed.* **2011**, *50* (30), 6793–6795.

(21) Yan, R.; Sander, K.; Galante, E.; Rajkumar, V.; Badar, A.; Robson, M.; El-Emir, E.; Lythgoe, M. F.; Pedley, R. B.; Årstad, E. A One-Pot Three-Component Radiochemical Reaction for Rapid Assembly of ^{125}I-Labeled Molecular Probes. *J. Am. Chem. Soc.* **2013**, *135* (2), 703–709.

(22) Lu, Z.; Pham, T. T.; Rajkumar, V.; Yu, Z.; Pedley, R. B.; Årstad, E.; Maher, J.; Yan, R. A Dual Reporter Iodinated Labeling Reagent for Cancer Positron Emission Tomography Imaging and Fluorescence-Guided Surgery. *J. Med. Chem.* **2018**, *61*, 1636–1645.

(23) Lakouraj, M. M.; Ghodrati, K. A Facile and Convenient Method for the Conversion of Thioamides into Amides Using Pyridinium Hydrobromide Perbromide. *Monatshefte fur Chemie* **2008**, *139*, 549–551.

(24) Castañeda, L.; Wright, Z. V. F.; Marculescu, C.; Tran, T. M.; Chudasama, V.; Maruani, A.; Hull, E. A.; Nunes, J. P. M.; Fitzmaurice, R. J.; Smith, M. E. B.; et al. A Mild Synthesis of *N*-Functionalised Bromomaleimides, Thiomaleimides and Bromopyridazinediones. *Tetrahedron Lett.* **2013**, *54* (27), 3493–3495.

(25) Sahu, S.; Rani Sahoo, P.; Patel, S.; Mishra, B. K. Oxidation of thiourea and substituted thioureas: a review, *J. Sulfur Chem.* **2011**, 32(2),171-197.

(26) Li, L.; Han, B.; Wang, Y.; Zhao, J.; Cao, Y. Simple and Universal Signal Labeling of Cell Surface for Amplified Detection of Cancer Cells Via Mild Reduction. *Biosens. Bioelectron.* **2019**, 145, 111714.

(27) Tracking Peripheral Immune Cell Infiltration of the Brain in Central Inflammatory Disorders Using [Zr-89]Oxinate$_4$-labeled Leukocytes, https://clinicaltrials.gov/ct2/show/NCT03807973.

(28) Sato, N.; Stringaris, K.; Davidson-Moncada, J.K.; Reger, R.; Adler, S. S.; Dunbar, C.; Choyke, P. L.; Childs, R. W.; In-vivo tracking of adoptively transferred natural killer-cells in rhesus macaques using ^{89}Zirconium-oxine cell labeling and PET imaging. *Clin. Cancer Res.* **2020**, Feb 7 doi: 10.1158/1078-0432.CCR-19-2897. [Epub ahead of print].

(29) Badawi, R. D.; Shi, H.; Hu, P.; Chen, S.; Xu, T.; Price, P. M.; Ding, Y.; Spencer, B. A.; Nardo, L.; Liu, W.; Bao, J.; Jones, T.; Li, H.; Cherry, S. R. First Human Imaging Studies with the EXPLORER Total-Body PET Scanner, *J. Nucl. Med.* **2019**, 60(3), 299–303.

TABLE OF CONTENTS GRAPHIC